arXiv:0705.0065v1 [astro-ph] 1 May 2007

DISCOVERY OF THE PUTATIVE PULSAR AND WIND NEBULA ASSOCIATED WITH THE TEV GAMMA-RAY SOURCE HESS J1813−178

D. J. Helfand, E. V. Gotthelf, J. P. Halpern, F. Camilo, D. R. Semler
Columbia Astrophysics Laboratory, Columbia University, 550 West 120th Street, New York, NY 10027, USA

R. H. Becker
Department of Physics, University of California, Davis, 1 Shields Avenue, Davis, CA 95616; and Institute of Geophysics and Planetary Physics, Lawrence Livermore National Laboratory, 7000 East Avenue, Livermore, CA 94550

AND

R. L. White
Space Telescope Science Institute, 3700 San Martin Drive, Baltimore, MD 21218
To Appear in the Astrophysical Journal

ABSTRACT

We present a *Chandra* X-ray observation of G12.82−0.02, a shell-like radio supernova remnant coincident with the TeV gamma-ray source HESS J1813−178. We resolve the X-ray emission from the co-located *ASCA* source into a point source surrounded by structured diffuse emission that fills the interior of the radio shell. The morphology of the diffuse emission strongly resembles that of a pulsar wind nebula. The spectrum of the compact source is well-characterized by a power-law with index $\Gamma \approx 1.3$, typical of young and energetic rotation-powered pulsars. For a distance of 4.5 kpc, consistent with the X-ray absorption and an association with the nearby star formation region W33, the $2 - 10$ keV X-ray luminosities of the putative pulsar and nebula are $L_{PSR} = 3.2 \times 10^{33}$ ergs s^{-1} and $L_{PWN} = 1.4 \times 10^{34}$ ergs s^{-1}, respectively. Both the flux ratio of $L_{PWN}/L_{PSR} = 4.3$ and the total luminosity of this system predict a pulsar spin-down power of $\dot{E} > 10^{37}$ ergs s^{-1}, placing it within the ten most energetic young pulsars in the Galaxy. A deep search for radio pulsations using the Parkes telescope sets an upper-limit of ≈ 0.07 mJy at 1.4 GHz for periods $\gtrsim 50$ ms. We discuss the energetics of this source, and consider briefly the proximity of bright H II regions to this and several other *HESS* sources, which may produce their TeV emission via inverse Compton scattering.

Subject headings: stars: individual (CXOU J181335.1−174957, G12.82−0.02) — ISM: supernova remnant — stars: neutron — X-rays: stars — pulsars: general

1. INTRODUCTION

The HESS observatory has revolutionized the field of TeV gamma-ray astronomy, opening a new window onto the highest energy processes occurring in our Galaxy and beyond. Of the 21 Galactic TeV sources detected by *HESS* during the first two years of four-telescope operation, firm identifications have been made for only seven objects (*HESS* "A" class sources – Funk et al. 2006a). Of these sources, nearly all are associated with supernova products: four with bright pulsar wind nebula (PWNe – three of which contain detected young, energetic pulsars), and two with non-thermal shell-type supernova remnants (SNRs); the remaining object is associated with a high-mass X-ray binary system. There are five less secure associations with SNRs/PWNe (*HESS* "B/C" class sources). The remaining nine *HESS* sources have yet to be identified with a known object at any other wavelength.

An opportunity to study the origin of SNR TeV emission is provided by the coincidence of the unidentified TeV source HESS J1813−178 with a previously uncatalogued shell-type radio supernova remnant G12.82−0.02 (Brogan et al. 2005; Ubertini et al. 2005; Helfand et al. 2005). This low-surface-brightness, small-diameter ($\sim 2'$) remnant lies within the 1σ extent of HESS J1813−178 and is coincident with a bright *ASCA* X-ray source. The possibility that this source represented a third example

of a shell-type SNR producing non-thermal X-rays along with TeV gamma rays raised considerable interest; however, as noted by the above authors, the source of the high-energy emission could also be an energetic pulsar associated with this apparently young remnant. Helfand et al. (2005) noted the proximity of the star forming region W33 as a source of ambient photons for producing gamma-rays from inverse Compton scattering.

We report here on a *Chandra* high-resolution image of G12.82−0.02. The X-ray flux from the remnant is resolved into diffuse non-thermal emission that fills the interior of the radio SNR, and surrounds a bright non-thermal point source. In §2 we describe the *Chandra* observation of G12.82−0.02, as well as supporting data we have collected in other wavelength regimes. In §3, we discuss our interpretation of this system as a young, energetic rotation-powered pulsar associated with the radio remnant and powering a pulsar wind nebula[1]. We also consider the origin of TeV emission from this and other HESS sources, suggesting that the presence or absence of a high-intensity, local source of optical/IR photons may often be determinative in the production of a TeV source. In the following text we assume a distance to G12.82−0.02 of 4.5 kpc, as discussed in §3.1.

---

[1] While this paper was in preparation, Funk et al. (2006) submitted and posted a discussion of their *XMM* observations of HESS J1813−178 that reaches similar conclusions.
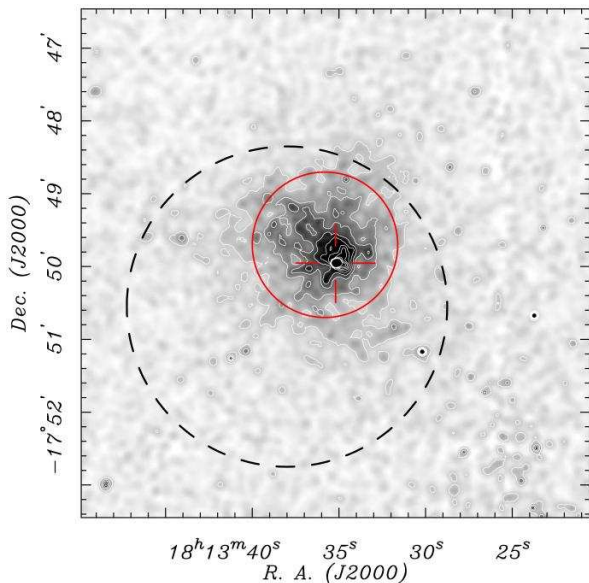
FIG. 1.— The 30 ks *Chandra* ACIS-I broad-band X-ray image of G12.82−0.02 smoothed and scaled to highlight the extended diffuse emission. The cross marks the location of the point source. The solid red circle ($r = 1'$) gives the mean size of the supernova remnant's radio shell and the dashed circle shows the 1σ extent of tev ($r = 2'.2$). This portion of the image contains 23 other source significant at the $\geq 3\sigma$ level (see Table 1), and represents 17% of the full ACIS-I field-of-view.

2. OBSERVATIONS AND RESULTS

2.1. *The Chandra X-ray Observation*

A 30 ks X-ray observation of SNR G12.82−0.02 was obtained on 2006 September 15 UT using the *Chandra* X-ray Observatory. Data were collected with the Advanced CCD Imaging Spectrometer (ACIS) in the focal plane, operating in the nominal full-frame TIMED/VFAINT exposure mode. This detector is sensitive to X-rays in the 0.3–12.0 keV energy range with a resolution of $\Delta E/E \sim 0.06$ FWHM at 1 keV. The imaging system offers an on-axis spatial resolution of $\sim 0''.5$, which is also the instrument pixel size. The *ASCA* source associated with G12.82−0.02 was positioned on the ACIS-I3 front-illuminated CCD and offset by $2'$ from the nominal aimpoint to allow any extended X-ray emission from the source to fall wholly on this one CCD. A total of 29.6 ks of live-time was accumulated with a CCD frame time of 3.241 s (given the 1.3% readout deadtime). No time filtering was necessary as the background rate was stable over the course of the observation. With a maximum count rate in a pixel of $< 0.004\,\mathrm{s}^{-1}$, photon pile-up can be safely ignored. We used the standard processed and filtered event data, with the exception that the level 2 event file was reprocessed to remove the pixel randomization, restoring a slightly sharper image. All data reduction and analysis was performed using the CIAO (V3.3.0), FTOOLS (V6.0.4), CALDB 3.2.3, and XSPEC (V12.2.1) X-ray analysis software packages.

As shown in Figures 1 and 2, the *Chandra* image of G12.82−0.02 resolves the *ASCA* source into diffuse X-ray emission that mostly fills the radio shell and peaks toward a bright unresolved point source, the brightest within the full $16' \times 16'$ ACIS-I 4-CCD field-of-view. This point source is offset from the geometric center of the radio remnant by $\approx 20''$. Near this source is a localized,

oval-shaped structure extending to the west/southwest (see Figure 2). It is clear from a radial profile centered on the point emission (Figure 3) that this excess emission is prominent out to $5''$ and disappears into the background at about $10''$. The radial profile is otherwise consistent with that of a point source when the large-scale diffuse emission filling the radio shell is taken into account. The overall morphology is highly reminiscent of a young, energetic pulsar within a structured pulsar wind nebula.

The highest radio surface brightness region of the shell lies along its western boundary, suggesting it has encountered a higher ambient density in this direction. Taking the possibility of asymmetric expansion into account, the location of the X-ray point source is consistent with the location of the supernova explosion. The offset of the point source from the center of the shell represents a distance of only ≈ 0.4 pc at the adopted distance of 4.5 kpc (see §3.1), implying $v \lesssim 385$ km s^{-1} if the remnant is $\gtrsim 10^3$ yr old.

To improve on the nominal *Chandra* astrometry, we registered the ACIS image using nine X-ray sources near G12.82−0.02 whose coordinates match with optical objects in the USNO-B1.0 Catalog (Monet et al. 2003 – typical uncertainty $0''.2$) to $< 1''$ initially. These calibrators and other field sources were identified and their coordinates measured using the CIAO software package source detection tool `wavdetect`. A fit of the X-ray-optical offsets, weighted by the positional uncertainties of each source, resulted in a mean correction of $+0''.01$ in R.A. and $-0''.34$ in decl., with a dispersion of $0''.3$ in radius, comparable to the statistical uncertainties in individual source positions. The final X-ray positions for the 75 sources that have a signal-to-noise ratio ≥ 3 are given in Table 1, along with the magnitudes of detected optical counterparts (see §2.3). The corrected position of the pulsar candidate (source #59) is R.A. = $18^\mathrm{h}13^\mathrm{m}35^\mathrm{s}.166$, decl. = $-17°49'57''.48$ (J2000) with a 1σ error radius of $\approx 0''.3$. These coordinates lie less than $1'$ from the maximum probability centroid of HESS J1813−178, and well within its 1σ extent radius of $2'.2$.

The morphology and location of the X-ray source indicates with all but certainty a young, energetic pulsar/PWN system; this conclusion is further supported by the following X-ray spectral analysis. We identify three regions from which to extract spectra: a) the point source CXOU J181335.1−174957, b) an inner nebula, and c) the greater PWN, which comprises the bulk of the diffuse emission. In the following we define each region and tally the extracted counts in the $2-10$ keV energy band, below which the spectra are highly attenuated due to the large column density (as determined by the spectral fitting below).

For the point-source spectrum, we extract a total of 864 photons from a $2''.0$ radius aperture centered on the source peak; the diffuse emission produces a negligible background (19 counts; $\approx 2\%$) in this region as determined by the counts in a concentric $2.5'' \leq r < 15''$ annulus. For the inner nebula we use a $6'' \times 8''$ elliptical extraction region centered at R.A. = $18^\mathrm{h}13^\mathrm{m}34^\mathrm{s}.89$, decl. = $-17°49'56''.9$ (J2000) with a position angle of $240°$. After accounting for the local background (28%) in a $1'$ diameter circle with the elliptical region removed, and excising the point source, this yields a total of 223
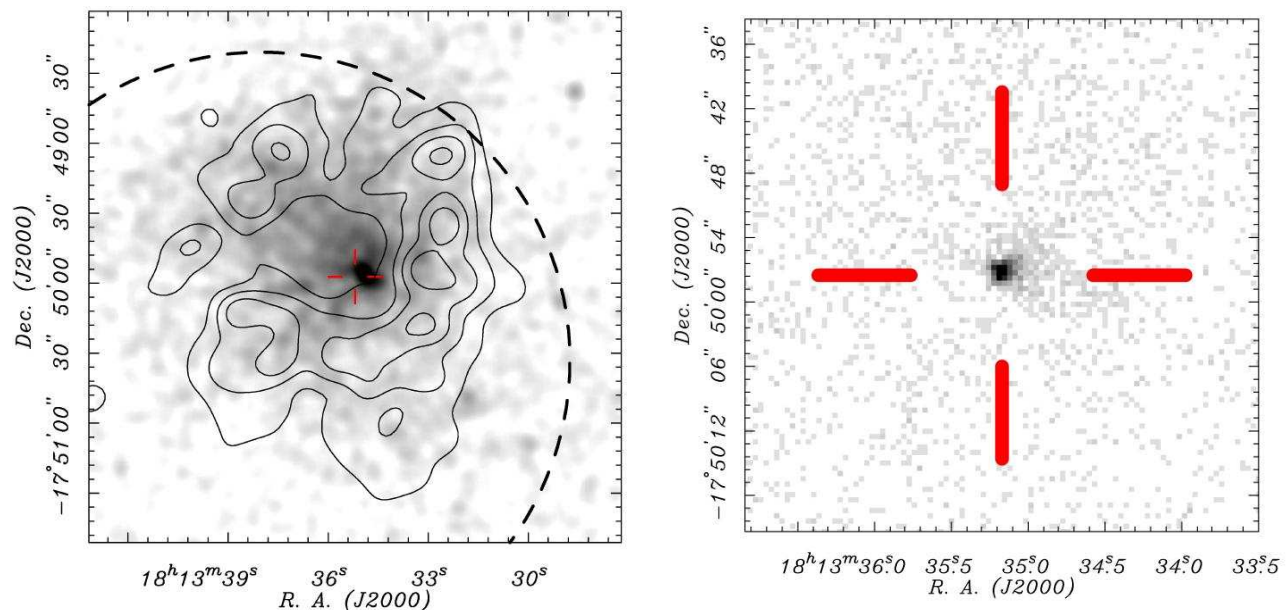
FIG. 2.— The *Chandra* resolved X-ray emission component from G12.82−0.02. *Left*: The broad-band, smoothed X-ray image of G12.82−0.02 with VLA radio contours overlaid; the point source, whose location is indicated by the red cross, was removed to highlight the diffuse emission. The dashed circle illustrates the 1σ extent of HESS J1813−178. *Right*: Zoom-in at full resolution of the X-ray image centered on the point source, a candidate pulsar. The intensity is scaled to highlight the point source and inner filamentary feature. The red cross is the same size (in arcseconds) and location in both panels.
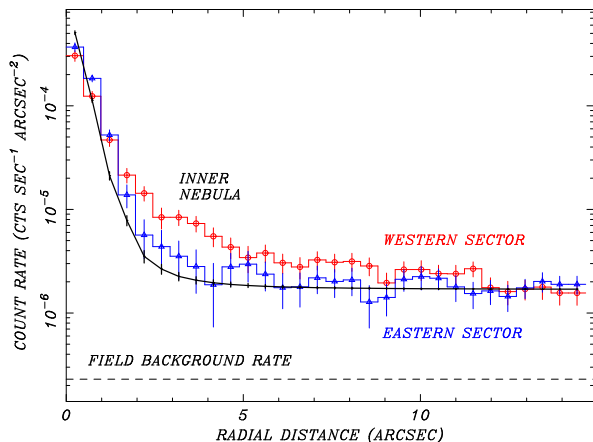
FIG. 3.— *Chandra* ACIS radial profiles around the candidate pulsar for the western (*red*) and eastern (*blue*) sectors compared to the point spread function (PSF; *black line*). The PSF is normalized to the peak of the emission and scaled vertically to match the data around $15''$ radius to highlight deviation from a pure point source due to the inner nebula emission, clearly evident in the western sector (see text).

photons. For the nebula as a whole, we define an $80''$ radius circle, offset from the point source and centered at R.A. $= 18^{\rm h}13^{\rm m}36^{\rm s}.50$, decl. $= -17°49'35''.6$ (J2000), encompassing the bulk of the nebula extent. With the point source and oval feature regions excluded, we collect a total of 6638 photons. The background for the PWN spectrum is extracted from a $56''$ radius aperture offset $2'.3$ due north of the source region and containing 1363 counts.

Spectra from each region were grouped with a minimum of 15 counts per spectral channel and fitted using the XSPEC software in the $2 - 10$ keV energy band; the results are summarized in Table 2 and Figure 4. The PWN emission is well-characterized (but not uniquely) by an absorbed power-law model with best-

fit photon index of $\Gamma = 1.3(1.1 - 1.6;$ 90% confidence interval), averaged over the nebula, and a hydrogen column density of $N_{\rm H} \approx 9.8(8.7 - 11) \times 10^{22}$ cm^{-2}, a relatively high value implying substantial absorption along the line of sight. The spectrum of the putative pulsar is fitted by a power-law model with the column density fixed to the value derived from the high-significance PWN spectrum. The best-fit model yields a surprisingly similar index, $\Gamma = 1.3 \pm 0.3$, not unlike that found for the Vela pulsar, and to be expected for a high-$\dot{E}$ rotation-powered pulsar (cf. Gotthelf 2003). The absorbed $2 - 10$ keV fluxes for the putative pulsar (PSR) and PWN are $F_{PSR} = 1.3 \times 10^{-12}$ ergs cm^{-2} s^{-1} and $F_{PWN} = 5.6 \times 10^{-12}$ ergs cm^{-2} s^{-1}, respectively. These results are consistent with the *ASCA* spectral measurements for the composite spectrum (e.g., Brogan et al. 2005). The spectral distribution of the inner nebula (IN) photons is not well-constrained, but a fit with the power-law model yields a somewhat flatter index than that of the PWN ($\Gamma = 0.4^{+0.4}_{-0.7}$), with a flux of $F_{IN} \sim 4 \times 10^{-13}$ ergs cm^{-2} s^{-1}.

The point-source flux is constant over the 30 ks observation. The ACIS frame time of 3.2 s does not permit a search for the signal of a typical rotation-powered pulsar in this observation. A search for slow pulsations by means of a fast Fourier transform (FFT) yielded no evidence of a signal with a 3σ upper-limit to the pulsed fraction of 27% for a Nyquist-limited sinusoidal period of $P > 6.5$ s. A constraint on shorter periods is provided by the *ASCA* data. A timing analysis revealed the source to have a constant flux over the 100 ks spanned by the 30 ks of net exposure; no periodic variability was detected in the period range 0.125 s to 1000 s (cf. Brogan et al. 2005). This is not surprising since the emission is dominated by the PWN and a pulsed signal would be washed out. Given the relative fluxes of the various components resolved by *Chandra* but blended by the *ASCA*

As part of a project to search for pulsar counterparts to a number of interesting radio sources described in Helfand et al. (2006), on 2005 September 8 we observed HESS J1813−178 with the ATNF Parkes telescope in NSW, Australia. Our pointing position, R.A. = $18^h13^m19^s.4$, decl. = $-17°54'46''$, was $6'.1$ away from the precise position of the subsequently identified *Chandra* source. We used for this search the central beam of the Parkes multibeam receiver operating at a central frequency of 1374 MHz, with 96 frequency channels spanning a total bandwidth of 288 MHz in each of two polarizations (see, e.g., Manchester et al. 2001). During the integration time of 30 ks, total-power samples were recorded every 0.25 ms to magnetic tape for off-line analysis.

We analyzed the data with standard pulsar searching techniques implemented in the PRESTO software package (Ransom 2001; Ransom et al. 2002). We searched the dispersion measure range 0–3344 cm^{-3} pc (twice the maximum Galactic DM predicted for this line-of-sight in the Cordes & Lazio 2002 electron density model), while maintaining close to optimal time resolution (scattering of the radio pulses due to multipath propagation is of no consequence here, being about 1 ms for the expected DM ~ 300 cm^{-3} pc at the distance of 4.5 kpc which is justified in §3.1). We first excised the worst of the radio frequency interference in the data, and searched for pulsars having a large range of duty cycles and spin periods between 0.5 ms and ~ 5 s. We also searched for pulsars whose spin period could have changed moderately during the observation (due either to very large intrinsic spin-down or a binary companion). The search followed very closely that described in more detail in Camilo et al. (2006). We did not identify any promising pulsar signal in this search.

Because of the $6'.1$ offset between our pointing position and the location of the X-ray pulsar candidate (§ 2.1), the sensitivity of our search was ≈ 0.7 that of an on-source search (the full-width at half-maximum of the telescope beam is $14'.4$). Using the standard modification to the radiometer equation for a conservative duty cycle for the pulsations of 10%, and accounting for a sky temperature at this location of 15 K, we were sensitive to long-period pulsars ($P \gtrsim 50$ ms) having a period-averaged flux density at 1.4 GHz of $S_{1400} > 0.07$ mJy, with the limit becoming progressively worse for shorter pulse periods. For a distance of ~ 4.5 kpc, this corresponds to a pseudo-luminosity limit of $L_{1400} \equiv S_{1400}d^2 \lesssim 1.4$ mJy kpc^2. This is nearly a factor of 3 above the detected L_{1400} for the young pulsar in 3C58 (Camilo et al. 2002a), which has the smallest known luminosity among young pulsars, but is comparable to or below that of other young, low-luminosity pulsars (see, e.g., Camilo et al. 2002b).

2.3. *Optical Observations*

The field containing G12.82−0.02 was observed on 2005 July 5 using the 2.4m Hiltner Telescope of the MDM Observatory on Kitt Peak, Arizona. A thinned, back-side illuminated SITe CCD with a spatial scale of $0''.275$ per $24\mu m$ pixel was used with an *R*-filter to cover a $9'.4$ field centered on G12.82−0.02 in seeing of $1''.5$. In Figure 5 we show a portion of the combined 18 minute exposure centered on CXOU J181335.1−174957. Taken under photometric conditions, the image was calibrated using
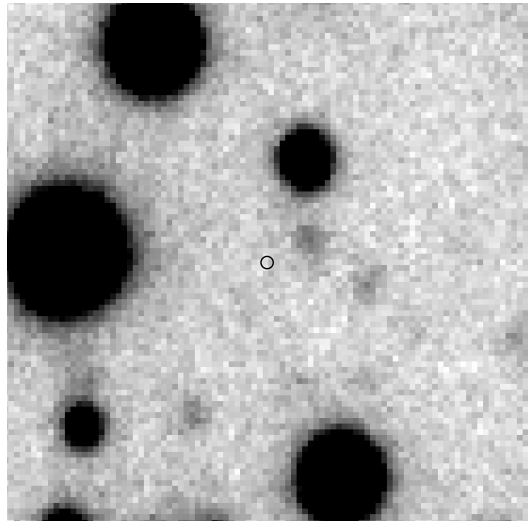

FIG. 5.— A portion of the *R*-band CCD image centered at the location of CXOU J181335.1−174957, obtained with the 2.4m Hiltner Telescope on 2005 July 5. The seeing is $1''.5$, and the 3σ limiting magnitude is $R = 23.4$. The 1σ error circle of radius $0''.3$ marks the location of the putative X-ray pulsar, R.A. = $18^h13^m35^s.166$, decl. = $-17°49'57''.48$ (J2000). North is up and east is to the left in this $25'' \times 25''$ display.
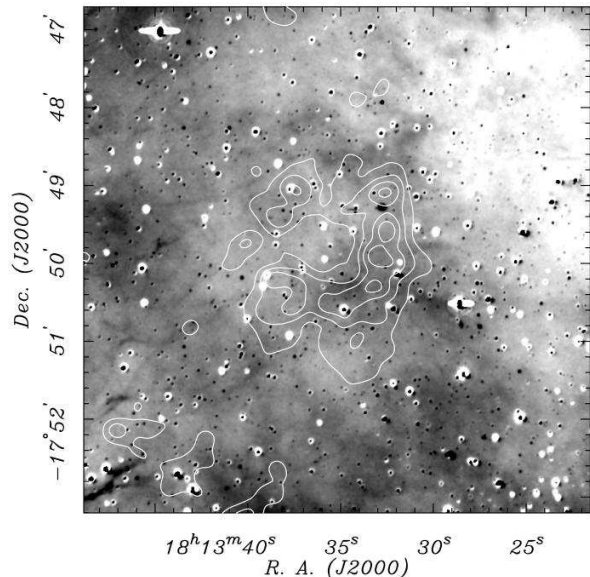
FIG. 6.— Hα image of the field of G12.82−0.02, obtained with the 2.4m Hiltner Telescope on 2005 July 5, with the VLA radio contours overlaid. Point-like artifacts from imprecisely subtracted and saturated stars remain.

Landolt (1992) standard stars. An astrometric solution for the image was derived in the reference frame of the USNO-B1.0 catalog (Monet et al. 2003) using 44 stars that have an rms dispersion of $0''.45$ about the fit. Since this is the same reference frame to which the X-ray coordinates were corrected, we can say confidently that there is no optical counterpart of CXOU J181335.1−174957 to a 3σ limiting magnitude of $R = 23.4$. Given the large column density to the source, the equivalent of ~ 20 mag of visual extinction, this limit is unconstraining. No counterpart is apparent in the 2MASS near-IR or Spitzer GLIMPSE (Benjamin et al. 2003) mid-IR images either.

We also obtained 72 minutes of exposure through a rest-frame Hα filter with a bandpass of 100 Å. A scaled

version of the R-band image was subtracted from the Hα image to highlight the diffuse emission by removing stars to the extent possible. Figure 6 shows the resulting Hα image, with the VLA radio contours of G12.82$-$0.02 superposed. While diffuse Hα emission is present throughout the image, there is no indication from its morphology that any of it is associated with G12.82$-$0.02. Again, given the extinction to the source, this null result is unsurprising.

We searched for likely optical counterparts to the other X-ray sources given in Table 1. R magnitudes were obtained from the USNO-B1.0 catalog or, for fainter or blended stars, from our own CCD image, which covers only part of the X-ray field. In this dense stellar field, it is possible that some proposed counterparts are chance coincidences, especially near the edge of the field where X-ray positions are less accurate. Bright sources #51 and #69 are evidently flare stars as seen from their X-ray light curves, although #51 does not have an optical counterpart to the very deep limit $R > 23.4$. Sources without optical counterparts generally have hardness ratio $> +0.2$, consistent with being AGN or other distant objects.

3. DISCUSSION

Our investigation of G12.82$-$0.02 with *Chandra* makes a compelling case that the X-ray emission from this remnant is dominated by the energy output of a young, rotation-powered pulsar. In this section we explore the energetics of this source and constraints on its properties that can be developed in the absence of a detection of pulsed emission. We also discuss the possible implications for the origin of TeV emission from other examples of supernova products.

3.1. *The Distance to G12.82$-$0.02*

The X-ray absorbing column density we derive here for both the putative pulsar and its PWN, $N_{\rm H} = 9 \times 10^{22}$ cm^{-2}, is consistent with that found earlier from the *ASCA* data (Brogan et al 2005; Ubertini et al 2005). Brogan et al. provide a thorough review of the data relevant to the source distance, including the molecular column density of $N({\rm H_2}) = 8 \times 10^{22}$ cm^{-2} to a distance of ~ 4 kpc in this direction, and the total H I column through the Galaxy at this longitude of 2×10^{22} cm^{-2}. Given that a distance of $4 - 5$ kpc is roughly half the way to the edge of the H I disk in this direction, the total X-ray absorption is easily explained if G12.82$-$0.02 lies at or just beyond 4 kpc. The source's non-detection at low radio frequencies is consistent with it lying in the vicinity of, or beyond, the giant star formation region W33 which resides $18'$ to the south at an estimated distance of 4.3 kpc. Given these data and the plausibility of finding a young, core-collapse remnant in a star formation region, we adopt a distance of 4.5 kpc.

3.2. *The X-ray Energetics*

That the putative pulsar is highly energetic is indicated by the large nebula-to-pulsar flux ratio of $F_{PWN}/F_{PSR} = 4.3$ in the $2 - 10$ keV energy band; only rotation-powered pulsars with spin-down energy loss rates above $\dot{E} \approx 4 \times 10^{36}$ ergs s^{-1} have a ratio this large or greater (Gotthelf 2003). Furthermore, the total 2–10 keV luminosity of $L_x = 1.74 \times 10^{34}$ $d_{4.5}^2$ ergs s^{-1} from

G12.82$-$0.02 corresponds to $\dot{E} \sim 10^{37}$ ergs s^{-1} according to the correlation of Possenti et al. (2002), placing this object among the Galaxy's ten most energetic pulsars. In particular, G12.82$-$0.02 bears a striking similarity to SNR G106.6+2.9, a radio shell undetected in X-rays that contains the energetic pulsar PSR J2229+6114 with $\dot{E} = 1.8 \times 10^{37}$ ergs s^{-1} and flux ratio $F_{PWN}/F_{PSR} = 9$ (Halpern et al. 2001).

3.3. *The origin of TeV Gamma-rays*

The gamma-ray luminosity of HESS J1813$-$178 at energies above 200 GeV is 4.4×10^{34} $d_{4.5}^2$ ergs s^{-1}, nearly identical to its $2 - 10$ keV X-ray luminosity. This is the highest L_{TeV}/L_x ratio for any of the confirmed PWN gamma-ray emitters; the ratios are 0.5 for PSR 1509–58, roughly 0.3 for SNR G0.9+0.1 and Vela X, and 0.06 for the Crab Nebula. Upper limits to the TeV flux from two other prominent young PWNe in the composite remnants SNR G11.2–0.3 and SNR G29.7–0.3 (Kes 75) can be derived from the HESS Galactic Plane survey (Aharonian et al. 2006); they also imply $L_{TeV}/L_x \lesssim 1$. As Funk et al. (2006) show, the TeV emission from G12.82$-$0.02 can be fitted simultaneously to the hard X-ray data from INTEGRAL (Ubertini et al. 2005) and the $0.5 - 10$ keV X-ray spectrum[3] with an inverse-Compton model, although a low-energy break in the electron spectrum is required to explain the absence of a radio counterpart to the PWN.

We regard the proximity of W33 as a likely explanation for the relatively high TeV flux from G12.82$-$0.02. We find it noteworthy that a number of HESS sources are found where high-energy particle accelerators are located near H II regions, while other such accelerators without proximate sources of low-energy photons are weak or undetected at TeV energies. For example, the Crab Nebula has the lowest L_{TeV}/L_x for a PWN observed to date and lies more than $5°$ from the Galactic plane; likewise, Kes 75, an isolated SNR housing a very young and energetic pulsar but with no nearby H II regions, has $L_{TeV}/L_x < 0.2$ and is undetected by HESS. On the other hand, SNR G0.9$-$0.1 near the Galactic Center, PSR 1509$-$58 near the H II region G320.5$-$1.4, and G12.82$-$0.02 near W33 are all easily detected.

In addition, HESS J1640$-$465 is a new PWN candidate associated with the shell-type SNR G338.3$-$0.02 and is adjacent to a bright H II region (Funk et al. 2007). Those authors quote a $\Sigma - D$ distance for this remnant of 8 kpc, and therefore suggest that it is unassociated with the H II region, whose kinematic distance places it at 3 kpc. However, the $\Sigma - D$ relation is notoriously unreliable (Green 2005) and the 8 kpc distance would imply that HESS J1640$-$465 is considerably more luminous than the Crab Nebula, whereas a 3 kpc distance would imply $L_{TeV} \sim 2.5 \times 10^{34}$ ergs s^{-1}, similar to the other PWN detected to date. In addition, the source HESS J1834$-$087, coincident with the shell-type SNR G23.3$-$0.3, also lies within $9'$ of a bright H II region, while the historical remnant SN1006, the first SNR from which hard X-ray synchrotron flux was detected, has not been seen at TeV energies despite an intensive search (Aharonian et al. 2005); it lies over $14°$ from the Galac-

---

[3] Note that the X-ray fluxes in their Figure 6 should be reduced by about 20% to account for the fraction of the emission originating in the pulsar itself.

tic plane. This accumulating anecdotal evidence suggests that a systematic evaluation of the local optical/IR flux in the vicinity of known particle accelerators might point the way to detecting more TeV sources. *GLAST* will be invaluable for distinguishing between leptonic and hadronic TeV emissions mechanisms (e.g., Funk 2007); the evidence adduced here suggests the inverse Compton mechanism may be preferred for the majority of HESS detections.

REFERENCES

Aharonian, F., et al. 2005, A&A, 437, 135
Aharonian, F., et al. 2006, ApJ, 636, 777
Benjamin, R. A., et al. 2003, PASP, 115, 953
Brogan, C. L., Gaensler, B. M., Gelfand, J. D., Lazendic, J. S., Lazio, T. J. W., Kassim, N. E., & McClure-Griffiths, N. M. 2005, ApJ, 629, L105
Camilo, F., et al. 2002a, ApJ, 571, L41
Camilo, F., Manchester, R. N., Gaensler, B. M., & Lorimer, D. R. 2002b, ApJ, 579, L25
Camilo, F., Ransom, S. M., Gaensler, B. M., Slane, P. O., Lorimer, D. R., Reynolds, J., Manchester, R. N., & Murray, S. S. 2006, ApJ, 637, 456
Cordes, J. M., & Lazio, T. J. W. 2002, preprint (astro-ph/0207156)
Funk, S. 2007, 36th COSPAR Scientific Assembly, 36, 120
Funk, S., et al. 2006, A&A, submitted (astro-ph/0611646)
Funk, S., Hinton, J. A., Puehlhofer, G., Aharonian, F. A., Hofmann, W., Reimer, O., & Wagner, S. 2007, ApJ, submitted (astro-ph/0701166)
Green, D. A. 2005, Memorie della Societa Astronomica Italiana, 76, 534

Gotthelf, E. V. 2003, ApJ, 591, 361
Halpern, J. P., Camilo, F., Gotthelf, E. V., Helfand, D. J., Kramer, M., Lyne, A. G., Leighly, K. M., & Eracleous, M. 2001, ApJ, 552, L125
Helfand, D. J., Becker, R. H., & White, R. L. 2005 (astro-ph/0505392)
Helfand, D. J., Becker, R. H., White, R. L., Fallon, A., & Tuttle, S. 2006, AJ, 131, 2525
Landolt, A. U. 1992, AJ, 104, 340
Leahy, D. A., et al. 1983, ApJ, 272, 256
Manchester, R. N., et al. 2001, MNRAS, 328, 17
Monet, D.G., et al. 2003, AJ, 125, 984
Ransom, S. M. 2001, PhD thesis, Harvard University
Ransom, S. M., Eikenberry, S. S., & Middleditch, J. 2002, AJ, 124, 17
Ubertini, P., et al. 2005, ApJ, 629, L109